Marine and Petroleum Geology 146 (2022) 105930

Contents lists available at ScienceDirect

Marine and Petroleum Geology

journal homepage: www.elsevier.com/locate/marpetgeo

Preserved eolian bedforms control reservoir heterogeneity: Characterization and modeling workflow for the Avilé Member, Neuquén Basin, Argentina

Agustín Argüello Scotti [a,b,*], Mortaloni Matías [a], Luis Martino [a], Gonzalo Diego Veiga [c], Joaquín Pérez Mayoral [c]

[a] YPF S.A.; Macacha Güemes #515, Buenos Aires, Argentina
[b] University of Bergen, Department of Earth Science, 5020, Bergen, Norway
[c] Centro de Investigaciones Geológicas (CONICET-UNLP); Diagonal 113 #275, La Plata, Argentina

ARTICLE INFO

Keywords:
Eolian sedimentology
Reservoir modelling
Neuquen Basin
Reservoir characterization

ABSTRACT

Under certain conditions, most commonly abrupt flooding events, entire eolian bedforms can be incorporated into the geological record. Sediment that was essentially 'in transport' within these bedforms at the time of preservation has a distinct sedimentary architecture compared to that of *sensu stricto* accumulated intervals. Despite this, while the preservation of bedforms has been readily documented from outcrop and subsurface eolian successions, stratigraphic intervals corresponding to these bedforms have rarely been identified and separated from accumulated intervals. The impact of capturing and representing bedform intervals in reservoir models has therefore not been explored. The Avilé Member (Neuquén Basin, Argentina) is a prolific oil reservoir of eolian origin in which both bedforms and accumulated intervals are documented. The aim of this study is to use the Avilé Member record at the Puesto Hernández oilfield to develop a workflow to identify, characterize, map and model discrete eolian bedform and accumulated intervals in a subsurface scenario. Characterization of the unit's geometry, sedimentary facies, and petrophysics was carried out from seismic, wireline log and core analysis. The development of a conceptual model of the accumulation system and its evolution allowed the identification of bedform and accumulated intervals. Precise mapping of these intervals required the development of a geometrical method, based on correlating interdune lows and using a *datum* surface to provide for an approximation to the ancient accumulation surface. A zoning scheme conditioned by the intervals was tested against a simple, 'one-zone' model, to determine its effectivity in separating discrete heterogeneity zones. The model was also tested in a dynamic simulator to history match the field production and analyze its impact in dynamic reservoir simulation. This example serves as a valuable reference to illustrate how eolian bedforms and accumulated intervals may be identified, characterized, and modelled in subsurface scenarios around the world.

1. Introduction and aims

The preservation of eolian bedforms (usually dune and megadune scale) in the geological record is a relatively common phenomenon, widely documented both in outcrop and subsurface examples worldwide from different geological eras (Glennie and Buller, 1983; Clemmensen, 1989; Benan and Kocurek, 2000; Jerram et al., 2000; Scherer, 2002; Strömbäck and Howell, 2002; Rodriguez López et al., 2014). These deposits are usually formed due to rapid flooding of a dune field by continental or marine waters, or lava flows in some cases, putting the bedforms below a regional level of erosion. These bedforms provide a snapshot of the sedimentary system at a certain time, preserving sediment that was essentially in transport at the time and had not been yet accumulated (*sensu* Kocurek, 1999).

In his theoretical framework, Kocurek (1999) defined accumulation and preservation as two independent stages in the formation of the eolian record. Accumulation is defined as the passage of sediment from above to below the accumulation surface, an imaginary surface that links interdune troughs and separates sediment in transport from accumulated sediment (Middleton and Southard, 1984; Mountney, 2012).

* Corresponding author. University of Bergen, Department of Earth Science, 5020, Bergen, Norway.
E-mail address: agustin.scotti@uib.no (A. Argüello Scotti).

https://doi.org/10.1016/j.marpetgeo.2022.105930
Received 14 July 2022; Received in revised form 9 September 2022; Accepted 19 September 2022
Available online 22 September 2022

Preservation on the other hand, is a stage in which the body of strata is put below the regional baseline of erosion (Kocurek and Havholm, 1993). Accumulation of eolian strata is no guarantee of preservation (Kocurek, 1999) as their likeliness to de deflated or eroded is very high unless they are buried beneath yet additional sediments. In this context, a preserved succession of eolian facies containing bedforms involves a certain rock interval above the ancient accumulation surface, which was never accumulated *sensu* Kocurek and Havholm (1993) (Fig. 1) and that we refer to in this paper as preserved bedform intervals, or non-accumulated intervals.

The preserved bedform interval's deposits have a sedimentary architecture which is expected to be very different from accumulated intervals. Accumulated intervals are generated via bedform climbing, which occurs at very low angles in eolian dune and megadune systems (Kocurek, 1981; Rubin and Hunter, 1982; Mountney and Howell, 2000; Mountney, 2012). As a result, only the very lowermost parts of the migrating bedforms are incorporated into the accumulation. On the contrary, when bedforms are preserved, most of their deposits are incorporated into the record, including their upper sectors. In these cases, the architectural complexity that is usually found when studying modern dunes (McKee, 1979, Bristow et al., 1996, Bristow et al., 2000) is transferred to the geological record of the preserved bedform interval (Argüello Scotti and Veiga, 2019; Mountney et al., 1999). Interdune facies, which provide for a major source of heterogeneity in the geological record, occur at the accumulation surface and are only found in the accumulated interval, never within the preserved bedform interval. Dune collapse and mass wasting deformation which are to be expected in preserved bedform intervals (preservation by flooding) constitute relevant heterogeneities (Rodríguez-López and Wu, 2020; Ford et al., 2016). As a result, accumulated and non-accumulated intervals are expected to represent very distinctive 'styles' of sedimentary heterogeneity, even when generated by the same bedform type and scale.

Eolian successions usually form excellent conventional subsurface reservoirs. As a result, they are of great interest in hydrocarbon and water extraction and CO_2 storage, among others (Rodriguez López et al., 2014). As pointed out before, eolian reservoirs with documented preserved topography are abundant worldwide, including the Rotliegend Group in the North Sea (Howell and Mountney, 1997; Strömbäck and Howell, 2002) and the Norphlet Sandstone in the Gulf of Mexico (Ajdukiewicz et al., 2010). In the Neuquén Basin alone, 3 major oil reservoir units of eolian origin (Avilé Member, Troncoso Member, Tordillo Formation) have documented cases of bedform preservation (Dajczgewand et al., 2006; Argüello Scotti and Veiga, 2015; Valenzuela, 2002; Cevallos, 2005). Expected differences in sedimentary facies and architecture between accumulated and non-accumulated sections of these successions suggest that their representation in subsurface models may be essential to capture reservoir heterogeneity in reservoir models.

The Avilé Member at the Puerto Hernandez field provides an excellent opportunity to study an eolian succession in the subsurface involving accumulated and non-accumulated eolian intervals, in a context of an onshore mature field with relatively abundant, high-quality information. Since the first discovery wells from this unit were drilled in the late 1970s, information from seismic, regular and closely spaced wellbores, and cored sections has been acquired (Argüello, 2011). However, no detailed studies about the sedimentology and stratigraphy of the eolian succession and it's preserved bedforms have been published from this area. The aim of this study is to use the Avilé Member in the Puesto Hernandez Field to develop a workflow to characterize, identify, map and model discrete eolian bedform and accumulated intervals in a subsurface scenario. In addition, the remaining potential for enhanced oil recovery of residual oil at the Avilé in this and surrounding fields adds local value to this kind of detailed modeling study.

2. Geological setting

The Neuquén Basin has been described as a back arc depression which developed over the west margin of Gondwana from the Upper Triassic to the early Paleogene, across a complex tectonic history (Howell et al., 2005; Franzese et al., 2003). It had a roughly triangular shape and was bounded by a volcanic arc to the west and stable areas to the northeast and southwest (Fig. 2). During the Lower Cretaceous, this basin is considered to have been subject to stable thermal subsidence in what is referred to as its sag stage (Mitchum and Uliana, 1985). During this stage, the basin formed an embayment connected to the proto–Pacific Ocean and accumulated thick marine deposits punctuated by non-marine lowstand wedges, which represent sudden sea level falls (Legarreta, 2002).

The Avilé Member of the Agrio Formation (Weaver, 1931) forms part of one of such lowstand wedges (Legarreta, 2002, Veiga et al., 2007). The unit is broadly characterized as thin (usually less than 100 m thick) but widespread, dominantly siliciclastic, and related to non-marine accumulation (Veiga et al., 2002). It typically overlies marine facies of the Pilmatué Member (Fig. 3), bounded by a net erosive regional surface interpreted as a major sequence boundary (Leanza, 2009). The Avilé is capped by the generally offshore marine facies of the basal section of the Agua de la Mula Member, across a sharp and regional transgressive surface. According to detailed marine biostratigraphy in the overlying and underlying units the Avilé Member is considered to be Hauterivian

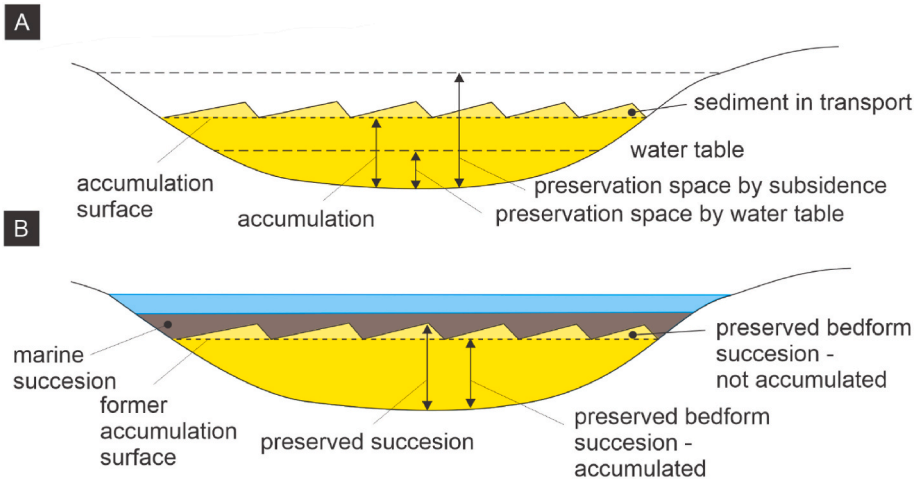

Fig. 1. Diagrams showing the components of accumulation and preservation in: (A) a dry dune system (modified from Kocurek and Havholm, 1993) and (B) the same system after sudden or 'catastrophic' flooding.

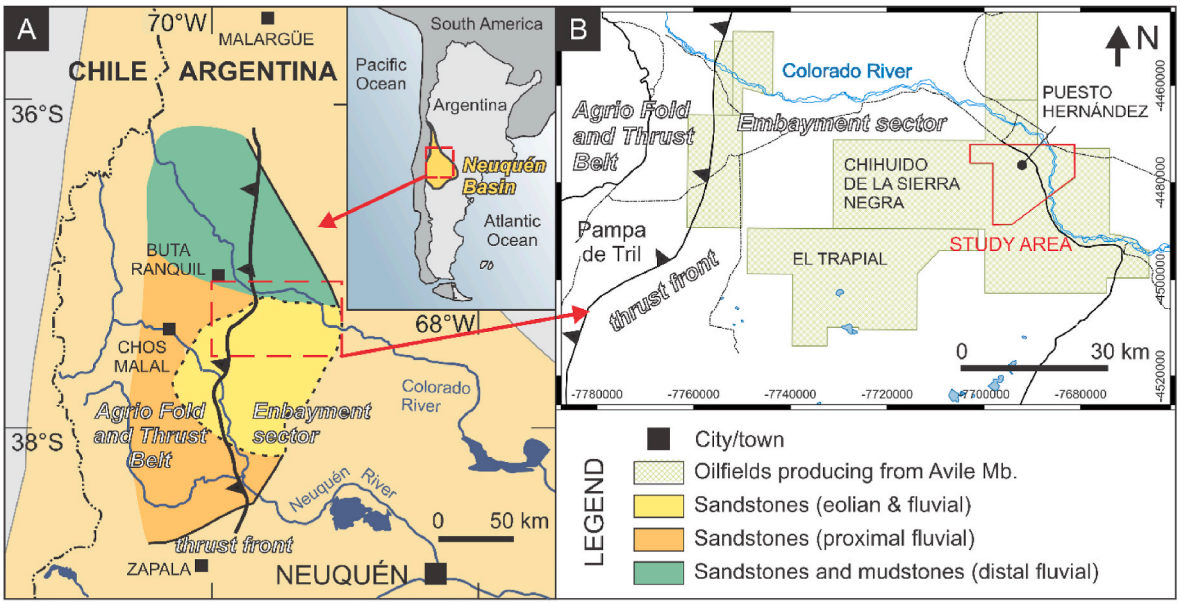

Fig. 2. Neuquén Basin and study area. (A) Map of the central-northern Neuquén Basin with the extent and sedimentary domains recorded in the Avilé Member according to Glennie and Buller, 1983). (B) Location of the Puesto Hernandez oil field, and other localities mentioned in the text.

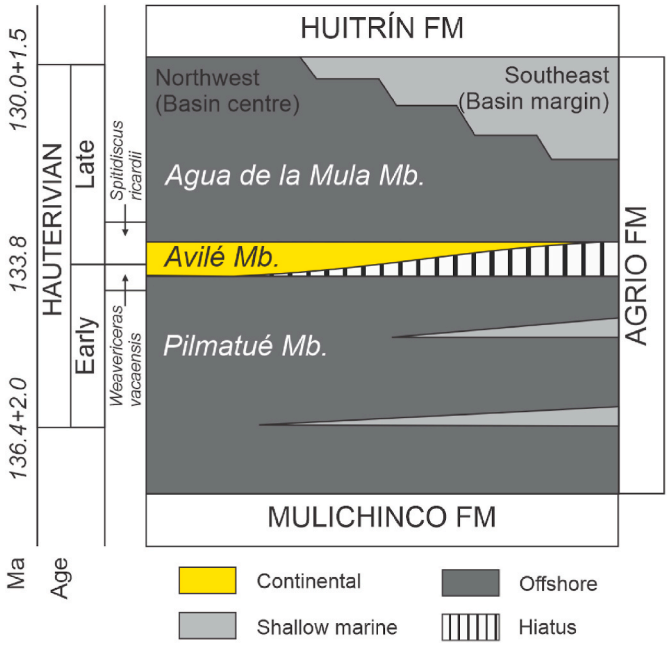

Fig. 3. Chronostratigraphy of the Cretaceous units in the Neuquén Bain and their broad depositional systems.

in age (Pramparo and Vokheimer, 2014). The unit crops out across the Andean region in the west, while it's found in the subsurface in the Embayment Sector to the east of the Agrio Fold and Thrust Belt (Fig. 2)

A variety of detailed studies of the Avilé Member, especially in outcrop sectors, have identified a suite of accumulation systems that include sandy and braided fluvial, mixed load meandering fluvial, open and hypersaline lacustrine, and eolian (Veiga et al., 2007, 2011). The deposits of the latter prevail in the easternmost outcrops, and into the subsurface sector (Fig. 2A). Detailed characterization of the vertical complexity of the unit at outcrop exposures and the inferred interaction between eolian and fluvial systems was presented by Veiga et al. (2002) at the Pampa de Tril locality (Fig. 2B). Although no preservation of eolian topography is registered in the outcrops, there are indications of such preservation in the subsurface sector. The study of Dajczgewand et al. (2006) suggests the presence of preserved eolian bedforms in the Avilé Member at the El Trapial Field (Fig. 2B), from seismic amplitude maps. Abrupt and regular lateral thickness variations of the whole unit, pointing towards the presence of preserved topography, are reported in the Avilé Member at most of the easternmost fields.

The Puesto Hernandez Field is located in the northernmost edge of the Neuquén Province, on the southern margin of the Colorado River (Fig. 2). Light oil was discovered in the field from the Avilé Member in 1968, rapidly becoming one of the most productive fields in the Neuquén Basin (Argüello, 2011). In the late 80's and early 90's, drilling of infill wells and waterflood recovery were performed with success. Since then, production from the Avilé has dwindled, while focus shifted to other reservoir units in the field. In this area, the Avilé Member is mainly composed of fine to medium sandstones dominantly eolian in origin with excellent petrophysical properties (Valenzuela, 2002). The reservoir unit varies in thickness from 8 to 30 mts. Towards the north of the field sandstones thin out completely and towards the eastern sector their petrophysical properties are strongly affected by diagenesis, contributing to the formation of a mixed structural-stratigraphic trap in the area (Argüello, 2011).

3. Dataset and methods

The sedimentology of the Avilé Member was characterized by a classical facies and facies association analysis performed on 150 m of core from 15 wells. Grain texture, composition, and sedimentary structure were used to define lithofacies and interpret basic depositional processes. Facies associations were defined by identifying meter-scale successions with commonly occurring lithofacies, their bounding surfaces, and the thickness of such facies assemblages. These were interpreted to represent genetically related units of strata resulting from a suite of processes occurring in discrete domains of a depositional system. Clay volume was estimated from Gamma-ray logs and combined with density data (RHOB) to define electrofacies, in a way that matched facies associations as accurately as possible. This was performed in the 274 wells (out of 383) that had bulk density logs. Electrofacies were a useful tool to analyze potential facies associations distribution with a much more representative and evenly spread sampling.

The geometry and seismic properties of the unit were characterized

from a 3D seismic survey and stratigraphic markers from wireline logs. A total of 383 wells with basic logs (SP, GR, Res) were used for this purpose. Thickness variations of the unit were studied from maps generated by stratigraphic markers and compared to seismic amplitude and acoustic impedance maps. Stratigraphic horizons picked from the marine units above and below were used as *datums*. *Datums* were key to determine if thickness variations were related to geometry at the top or base of the unit, and therefore to relate them with eolian bedform topography preservation (Avilé Member top) or to sequence boundary topography (Avilé Member base).

From this characterization and the use of outcrop analogues, an integrated conceptual model of the sedimentology and stratigraphy of the Avilé Member was developed. A geocellular model taking into account those concepts was developed for history match and forecast evaluation. The details of the workflow, with particular emphasis on how the contrasting eolian intervals were zoned and modelled, are presented in the geocellular modelling section.

4. Facies analysis

7 lithofacies were identified within the Avilé Member (Fig. 4., Table 1) which were grouped into 4 facies associations -FA- (Fig. 5, Table 2): FA-A and FA-B are related to accumulation in continental dryland conditions, while FA-C and FA-D are related to deformation and reworking of eolian sand by the reestablishment of marine conditions following the transgressive event that drowned the dune system.

4.1. Facies association A: eolian dune deposits

It is by far the most abundant facies association in cores (90% of logged thickness in cores). It typically consists of 5–25-m-thick successions of alternating grainflow (Sg) and wind-ripple laminated (Sw), very well sorted medium-to fine-grained sandstones (Table 1, Fig. 4). In addition, massive medium-to fine-grained sandstones with gradual and diffuse boundaries to grainflow sandstones are typically found in this association, often associated to intense hydrocarbon stain. Typical upwards transitions in lamination or stratification from subhorizontal, to low-angle, to inclined are common and easy to identify in dipmeter and FMI logs and help define the occurrence and boundaries of cross-bedding sets. $CaCO_3$ nodules are common in all facies of this association. Sometimes these nodules are abundant and aligned with sedimentary structures. In other occasions, specially at some set boundaries, such carbonate cement can totally obtrude the sandstone for a thickness of a few decimeters (Fig. 4).

4.1.1. Interpretation

This association reflects accumulation by migrating eolian dunes. Alternating grainflow, grainfall and wind-ripple laminated sandstones reflect deposition by migrating eolian dunes, via avalanching in dune slipfaces, settling of fine grains downwind of dune brinks, and by eolian wind ripple migration in dune plinths (Hunter, 1977; Kocurek and Dott, 1981). Massive facies showing transitional boundaries to grainflow and grainfall sandstones can be interpreted being originally deposited by the same processes as the latter and that the structure is just not visible due to hydrocarbon stain, diagenesis, or just the amalgamation of individual avalanche flows of very well sorted sand (Howell and Mountney, 2001). Gradual upwards increase in bedding dip angle indicates transition from plinth to slipface as the dune migrated, depositing a cross-bedded set (Besly and RomainMountney, 2018). The occurrence of thick cemented facies (Sc) at some set boundaries gives a strong indication of the presence of high-hierarchy surfaces. These could be attributed to deflation, very likely down or close to the water table, which could have promoted the formation of cemented horizons (Kocurek, 1981). These are therefore taken as a strong indication of the presence of Stokes' Surfaces or

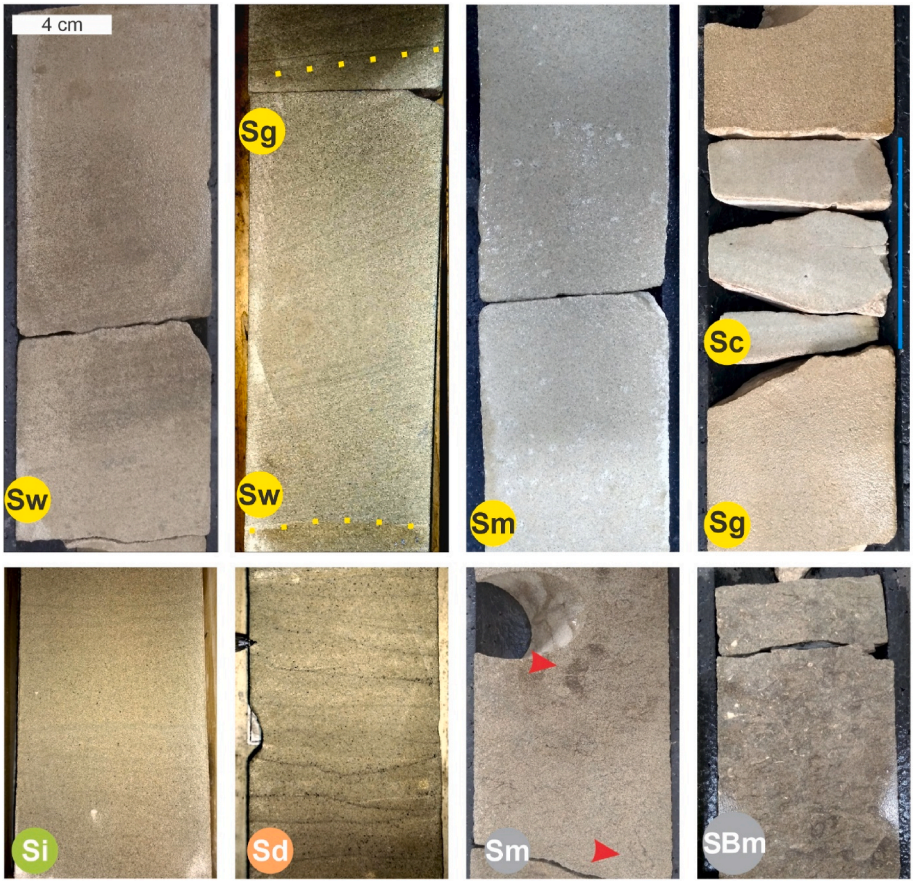

Fig. 4. Examples of most commonly occurring lithofacies in the Avilé Member (see Table 1 for lithofacies code reference). Color in the boxes indicate Facies Association (Yellow: FA-A; Green: FA-B; Orange: FA-C; Grey: FA-D). Blue line in facies Sg at the higher right indicate the vertical extent of a cemented horizon. Red arrows in facies Sm in the lower row indicate de presence of burrows and bioturbation. (For interpretation of the references to color in this figure legend, the reader is referred to the Web version of this article.)

Table 1
Lithofacies identified for the Avilé Member from cores.

%	Code/Name	Texture	Sedimentary structure	Basic dynamic interpretations
35	**Sg** Sandstone; grainflow	Medium to fine sandstone very good sorting	Inclined (10–25°) strata few cm in thick (1–6 cm), occasionally bounded by mm thick laminae	Grain avalanches over lee side of dunes, coupled with grain fall of fine grains from flow separation at the brink of dunes
25	**Sw** Sandstone; windripple	Medium to fine sandstone, good sorting	Low-angle (5–10°) to subhorizontal (<5°) laminae, up to 1 cm thick. Bimodal clast segregation	Migration of wind ripples over inclined to low angle surfaces
2	**Sl** Sandstone; low-angle stratification	Medium to fine sandstone, good sorting	Low-angle (5–10°) stratification	Tractive accumulation by unidirectional water currents, probably related to high regime flow bedforms
25	**Sm** Sandstone, massive	Medium to fine sandstone, good sorting	Massive	Lack of observable structure due to diagenesis or oil stain coupled with good grain sorting. Loss of original structure due to soft sediment deformation. Sudden accumulation by sediment gravity flows
2	**SBm** Bioclastic sandstone, massive	Medium to fine sandstone, moderate sorting, muddy matrix	Massive	Sediment gravity flows, loss of sedimentary structure by bioturbation
3	**Si** Sandstone, irregular lamination	Medium to fine sandstone, moderate sorting, muddy matrix	Irregular lamination, wrinkle lamination	Accumulation over damp surfaces and formation of wrinkles and warts and presence of haloturbation processes
3	**Sd** Sandstone, deformed	Medium to fine sandstone good sorting	Convolute structure of turned or deformed stratification-lamination of Sg and Sw facies	Soft sediment deformation of eolian facies by water or air scape
5	**Sc** Sandstone, cemented	Medium to fine sandstone, pores filled with cement	No preserved structure	calcite- and dolomite precipitation at bed boundaries. Likely related to early diagenesis and incipient duricrust-caliche formation

Super-Surfaces (Fryberger et al., 1988; Kocurek, 1988) in the studied section.

4.2. Facies association B: water-lain to damp deposits

This is the least-abundant association observed in core. It usually consists of few decimeters' thick successions of moderately sorted fine-grained sandstones with a silty matrix and wrinkle-lamination (Si, Fig. 4) and low-angle cross-stratified to sub-horizontal stratified medium-grained sandstones (Sl). These successions are usually interbedded with FA-A, bounded by net contacts, and are more abundant and thicker towards the lowermost meters of the Avilé Member. Furthermore, these are very frequently well-cemented by $CaCO_3$ nodules.

4.2.1. Interpretation

This association represents deposition in damp and wet conditions. Successions dominated by wrinkle laminated facies represent eolian accumulation by adhesion in damp surfaces under the influence of the water table's capillary fringe (Kocurek and Fielder, 1982; Fryberger et al., 2011). Low-angle cross-stratified and sub-horizontal stratified sandstones likely represent the deposition by dominantly unidirectional currents of water, likely by high-regime low-depth flows (Fielding, 2006). Considering their interbedding with FA-A, this facies association could be attributed to damp to wet interdune accumulation. However, they can also be interpreted as very poorly developed ephemeral fluvial systems in cases where the Avilé Member's dunes were deflated down to, or close, to the water level (Kocurek, 1981). If that were the case, they could be indicating the position of Stokes Surfaces or Super-Surfaces.

4.3. Facies association C: soft sediment deformed deposits

This facies association is mainly composed by well-sorted sandstones of convolutedly folded facies which result from the deformation original eolian sedimentary structures of FA-A, sometimes also associated with massive sandstone facies. Within this association is also common to find irregular shaped, very-fine grained sandstone laminae that closely resemble dish structures (Sd, Fig. 4). Successions of FA-C are found typically interbedded with FA-A, bounded by transitional contacts, and are more common towards the top of the unit.

4.3.1. Interpretation

This association reflects a suite of soft deformation processes of eolian sediment that is likely the result of marine flooding. Deformed and convolute bedding, and dish structures are typically found associated and are related to the sudden escape of water or pockets of air trapped within the sand (Lowe and LoPiccolo, 1974). This suite of processes and their associated structures are very much expected when eolian dunes are flooded and changes in pore pressure related to saturation and pockets of trapped air, triggers sudden deformation of eolian strata (Strömbäck et al., 2005).

4.4. Facies association D: marine reworking deposits

This association consist of few meters-thick successions of massive sandstone, and massive bioclastic sandstone beds. While most massive sandstones are well to moderately sorted, some poorly sorted sandstones characterized by a muddy matrix, bioclasts and bioturbation (Facies SBm, Fig. 4) are found at the top of the successions, towards the transition into the Agua de la Mula Member. Therefore, this association typically has a fining upwards trend. Successions of FA-D are always found in the uppermost meters of the Avilé Member and have sharp contacts with the underlying FA-A and the overlying stratigraphic unit. Sharp contacts between massive beds within the succession are also usually observed (Fig. 4). $CaCO_3$ nodules are common.

4.4.1. Interpretation

Given the stratigraphic position of these successions, their sedimentary structures, and the occurrence of bioclasts and poorly sorted sandstones, it is likely that these are the result a combination of sub-aqueous sediment gravity flows and in-situ homogenization by bioturbation. Where bedding contacts are well observed, it is possible these deposits are the result of liquified flows. These flows would have been triggered by the water saturation of eolian dunes because of the transgressive event, reducing cohesion between grains and triggering sediment gravity flows (Lowe, 1976). As such, they were most likely

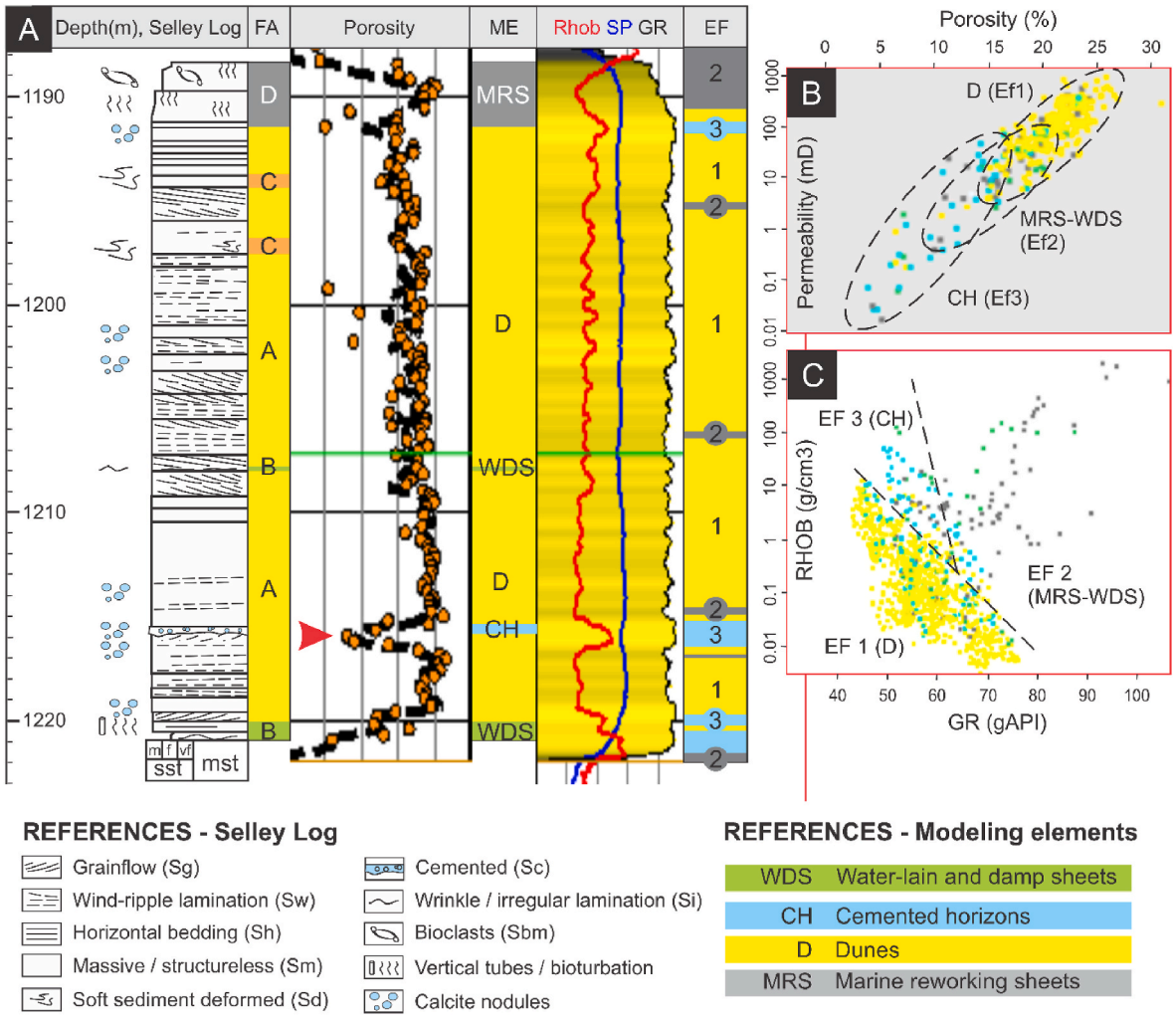

Fig. 5. Electrofacies model. A) Correlation between Selley log, Facies Associations (FA), Modeling Elements (ME), Wireline log readings (RHOB, GR, SP) and Electrofacies (EF) from one of the cored sections. The red arrow points out the impact of cemented horizons in reservoir properties and how it is captured by the Electrofacies Model. The green line that crosses the log at a depth of 1207 m is the interpreted position of the ancient accumulation surface. B) Porosity vs Permeability plot from plug data. Point color represents modeling elements. Dashed areas show how modeling elements represent porosity and permeability ranges and correlations. C) Plot of bulk density (RHOB) vs Gamma-ray (GR) wireline log readings at the position of plug samples, showing how modeling elements can be predicted by their log signature. Point color represents modeling elements. The fields marked by dashed lines were used to define electrofacies and spread them to coreless sections. (For interpretation of the references to color in this figure legend, the reader is referred to the Web version of this article.)

Table 2
Facies associations defined for the Avilé Member from cores.

Facies association	Lithology	Facies	Thickness (core)
A (Eolian dune deposits)	Well sorted, fine to medium grained sandstones	Sg, Sw, Sm	usually 5–20 m, up to 25 m
B (Water-lain to damp deposits)	Well to moderately sorted, fine to medium grained sandstones	Sl, Si, Sr, Ci	usually 10–20 cm, up to 1.5 m
C (Soft sediment deformed deposits)	Well sorted, fine to medium grained sandstones	Sm, Sd	usually less than 1 m, up to 2 m.
D (Marine reworked deposits)	Moderately to badly sorted, very fine to medium grained sandstones	SBm, Sm	up to 7 m

triggered by the same events that produced the deformation of eolian facies (FA-C). In outcrop examples, the distribution of these deposits with relation to the preserved dune topography suggest that they traveled downslope from crestal to flank and interdune sectors (as in the case of the flooded Troncoso Member dunes; Argüello Scotti and Veiga, 2015). Beds without clearly defined boundaries and with bioclasts and bioturbation would be related in turn with in-situ homogenization (Strömbäck et al., 2005).

5. Electrofacies and petrophysics

A total of 3 electrofacies -EF- were defined by a combination of wireline log signature, petrophysical properties, and facies analysis from cores (Fig. 5). EF-1 is defined by low API, low-density values (Fig. 5C). This electrofacies represents well-sorted, porous, and permeable facies of dunes elements (Fig. 5B), equivalent to FA-A and FA-C. EF-2 is characterized by high API with variable density values. It represents the more matrix-rich facies with impoverished petrophysical properties of water-lain or damp deposits of FA-B and marine reworked deposits of FA-D. EF-3 are clearly defined by low API, high-density values and represents cemented sandstone facies (Sc) with very unfavorable porosity and permeability values. These facies, although not linked to a specific facies association, conform a very important source of heterogeneity and are treated as a separate geological element (Table 3). This electrofacies scheme allowed the definition of 'modeling elements', characterized by an impact in reservoir properties, a recognizable log signature (Table 3) and a predictable geometry and dimensions.

Table 3
Simplified defining log signature of electrofacies (EF) and attempted equivalences to geological element and facies associations/lithofacies.

EF	Wireline log signature	Modeling element	FA - lithofacies
1	Low API, low density	Dunes	A C
2	Moderate to high API, low density	Water-lain to damp sheets	B
		Marine reworking sheets	D
3	Low Api, High density	Cemented horizons	facies Sc

6. Reservoir characterization

6.1. Seismic attributes

The Avilé Member is a thin unit in the study sector (5–35 m) and its expression in seismic is represented by one reflector. Clear and regular variations in seismic amplitude are apparent when looking at N–S oriented vertical slices (Fig. 6A). Amplitude variations are observed as a roughly regular pattern in a horizon slice, in which continuity of amplitude values is much stronger in E-W direction compared to N–S direction (Fig. 7A). The same pattern is observed in thickness maps of the unit produced from well data (Fig. 6B). An acoustic impedance map, corrected by unit thickness (Fig. 7B) will show the same pattern, even clearer than the amplitude map.

Variation of seismic amplitude values in the Avilé Member can be explained by their correlation to thickness values. However, acoustic impedance values were corrected by unit thickness, so their patten cannot be explained by mere variations in thickness. Given that the Avilé Member is almost entirely composed by sandstones, variations in acoustic impedance are likely linked to reservoir properties like porosity (Dolberg et al., 2000). Thick sectors (low acoustic impedance) would therefore be expected to have better overall reservoir properties in comparison to thin sectors (high acoustic impedance).

6.2. Reservoir geometry

A geometrical characterization based on a *datum* surface was used to determine the geometry of the top and basal surface and their relationship to unit thickness variation. The *datum*-referenced Avilé top boundary map (Fig. 8A) shows a relief in the order of 20 mts, which exactly matches the regular patterns in unit thickness and seismic attributes. Since the Avilé Member is almost exclusively conformed by sandstones, we descriptively call these regularly spaced thick sectors sandstone ridges. Three of such sandstone ridges are clearly observed in the study area, with a fourth one, not so clearly distinguishable, appears close to the west boundary of the study area. Ridge crests and lows have a spacing of around 1.5 km. Dip analysis (Fig. 8B) over the modelled top boundary surface indicates that the high and low sectors of the ridges were smooth (dip less than 1°) while the flanks were the steepest (up to 5–6°). Dip azimuth analysis on the other hand, indicated that the ridges are also symmetrical, given the percentages of total area under calculated dip azimuth classes (Fig. 8D).

Geometry of the top Avilé boundary clearly accounts for the variation in unit thickness. Since the Avilé top boundary is also regarded as a transgressive surface, with deep marine facies on top and eolian or marine reworking facies below, its geometry is best explained as the result of dune topography preservation from marine flooding. Size of the ridges suggest the preservation of megadune bedforms, while symmetric cross-sections suggest that megadunes were of linear morphology (Lancaster, 1995). As a result, high thickness areas are referred to as megadune sectors, while low thickness areas are referred to as interdune sectors..

6.3. Facies association and electrofacies distribution

Several vertical changes in facies associations were inferred from the cored sections. FA-B was almost always found interbedded with FA-A at the lowermost meters of the unit, while FA-C is interbedded with FA-A at the top of the unit. FA-D is found at the top, forming a discrete interval that caps the unit. FA-D is observed as a bell-shaped tendency in GR logs, very likely reflecting a thinning upwards trend (as observed in core). Vertical trends in electrofacies confirm this distribution across the study area (Fig. 9A). While EF-1 makes up for most of the unit, EF-2 is more common towards the topmost and lowermost meters. EF-3 is evenly distributed across the unit except for an increment in the lowermost meters, where is more frequent and forms thicker intervals. Lateral facies changes were evaluated in relationship with the unit's thickening and thinning (Fig. 9B). Nevertheless, no obvious variations were observed, except that the discrete interval of EF-2 at the top of the unit, shows a subtle increment in thickness in areas where the unit's overall thickness is thinner.

Facies association and electrofacies variations across the unit are subtle, and only justify separating FA-D as discrete interval at the top of

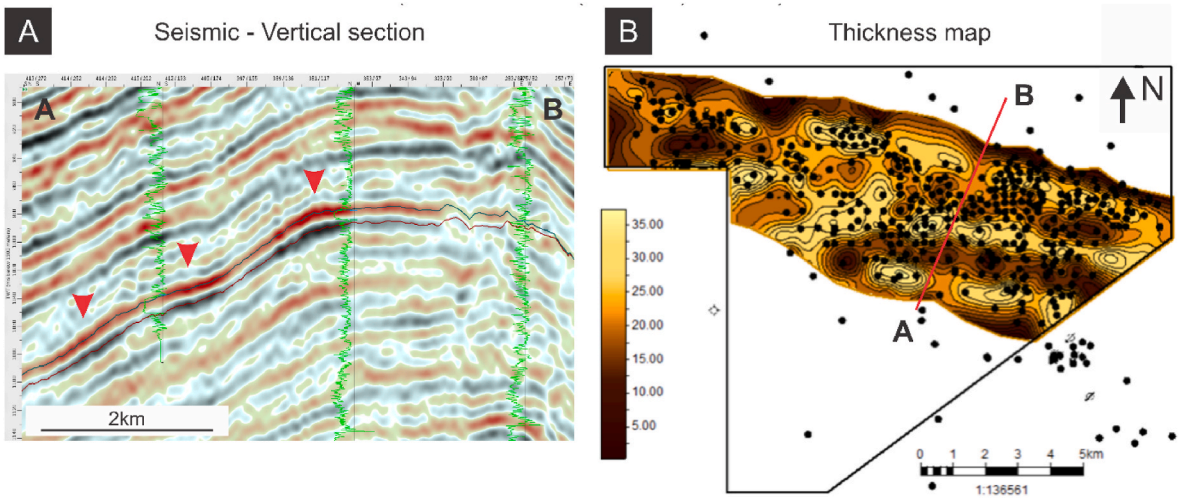

Fig. 6. Seismic section and thickness changes. (A) Northeast- Southwest oriented seismic section. Avilé horizons for base and top are marked by thin lines. Red arrows indicate peaks in horizon's amplitude. (B) Avilé thickness map from well data in the study area. Black dots in maps mark the position of wells. Black line marks the field's boundary. (For interpretation of the references to color in this figure legend, the reader is referred to the Web version of this article.)

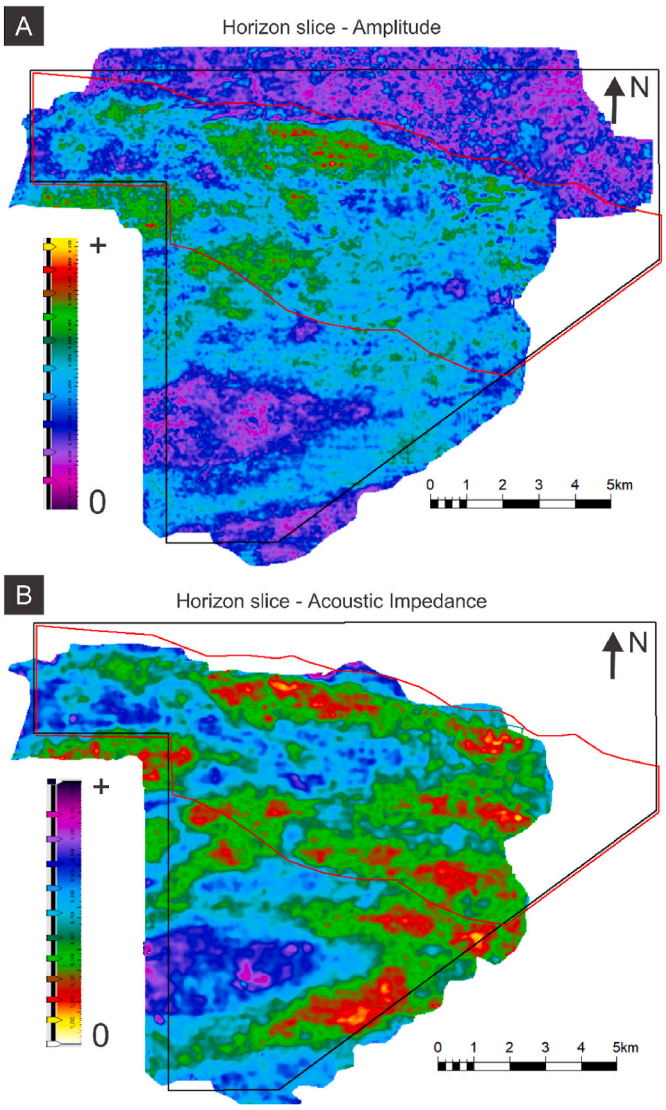

Fig. 7. Seismic attributes. The black line marks the field boundary and the red line the modelling area. (A) A horizon slice of Avilé Member showing variations in amplitude across the oilfield (B) Horizon slice of Avilé Member showing variations in acoustic impedance. See text for comparisons and discussion. (For interpretation of the references to color in this figure legend, the reader is referred to the Web version of this article.)

the unit. However, these subtle trends provide a lot of information which is useful to interpret seismic attribute variations and develop the geological conceptual model presented in the following section.

7. Conceptual model

7.1. Accumulation systems

FA-A, with subordinated interbedded FA-B and FA-C, are interpreted to be the record of an eolian dune system. A dominant eolian dune accumulation is also reported by earlier studies and in adjacent localities (Valenzuela, 2002; Argüello, 2011), and the easternmost outcrops of the unit (Veiga et al., 2002). The interbedding of water-lain to damp elements (FA-B) among eolian dune elements (FA-A) towards the base, could be interpreted in different ways. Firstly, they could be interpreted as the record of damp to wet interdune accumulation, indicating a damp to wet eolian dune system (Howell and Mountney, 1997). Alternatively, eolian accumulation might have been episodic, with episodes of deflation down to, or close, to the water table. In this scenario wet and damp deposits would be related to the development of incipient ephemeral fluvial systems after deflation and would not have any relationship with the dune system being wet or damp (Veiga et al., 2002). Unfortunately, a sedimentary architecture study would be needed to discern between these two scenarios, and this cannot be performed with the available data.

The characterization of eolian topography preserved at the top of the unit, provides important insights into the eolian accumulation system. Megadune linear bedforms are inferred from the scale (1,5 km wavelength) and symmetric cross section of the ridges (Lancaster, 1995). Since this bedform type is usually characterized by net transport parallel to the crest line (Fryberger and Dean, 1979), and considering paleocurrent readings (ranging from NE to SE, from dipmeter readings of cross bedding), it is most likely that sand was being transported from west to east. Since the unit does not completely thin out in the low thickness (interdune) sectors, and we are certain that eolian deposits predominate at these locations as well, we can infer that there was actual eolian accumulation (*sensu* Kocurek, 1999, *i.e.* a climbing set of dunes) in the study area before the start of the flooding. Therefore, we interpret that there is an accumulated interval in the lowermost meters, and a non-accumulated interval in the topmost meters. These would be two intervals which would hold subtle differences in facies, but big ones in sedimentary architecture. This is in concordance with the presence of water-lain or damp elements and cemented horizons in the lowermost meters, which would be expected from an accumulated interval, while the uppermost meters contain no water-lain facies, but soft sediment deformed facies as would be expected from the non-accumulated, preserved bedform interval.

The deposits of FA-D as a discrete interval on the top of the unit, is interpreted as the result of an establishment of a marine system, after flooding of the megadunes by the Neuquén Sea. Flooding and water saturation of the dunes below is also the likely trigger for the soft sediment deformation of eolian facies (FA-C). The thinning upward trend lack of facies that evidence wave action within this interval reflect rapid flooding of the area beneath wave base, and the rapid shift towards deep offshore or offshore transition accumulation conditions recorded in the lowermost Agua de la Mula Member.

7.2. Outcrop analogues

The Troncoso Member outcrops at Pampa de Tril make for an excellent analogue for the non-accumulated interval of the Avilé at Puesto Hernandez. Strömbäck et al. (2005) and later Argüello Scotti and Veiga (2019) studied the topography of linear megadunes preserved by flooding in this locality. These are very similar in recorded facies, bedform scale, megadune type and preservation mechanism (marine flooding) to those observed by the present study. Dip angle over the preserved megadune topography is also very similar, with nearly flat dune crests and interdunes, and inclined bedform flanks. Most importantly, marine reworked facies are observed to be nearly absent in crestal areas, thicken towards megadune flanks, and reach and fill interdune areas. This can explain why in the Avilé, the topmost interval of FA-D is thicker towards the interdune sectors, and partly explains why petrophysical conditions seem worse overall at these areas.

The Avilé Member outcrops at Pampa de Tril are a good analogue for the accumulated interval of the Avilé Member at Puesto Hernandez Field. The detailed study of Veiga et al. (2002) shows that the unit is characterized by a series of stages of eolian accumulation, separated by sharp, extensive, and planar surfaces, sometimes related to sand sheet or distal fluvial accumulation directly over them. Water-lain deposits over these surfaces become thicker in the uppermost section of the eolian record, which is in turn overlain by the deposits of a fluvial system. The interpretation for this sedimentary and stratigraphic architecture is that an eolian sand sea accumulation was characterized by a series of pulses, separated by stages of deflation down to the water table and the

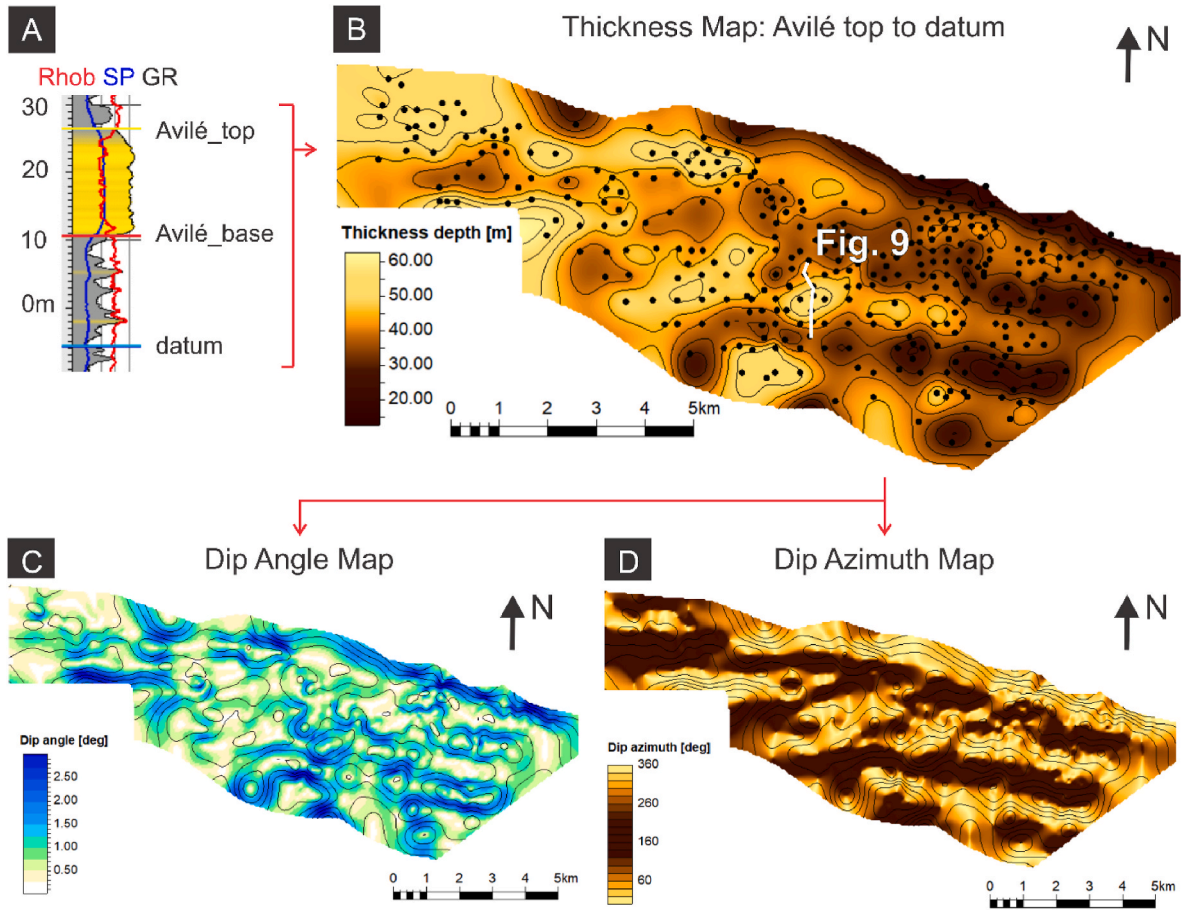

Fig. 8. Geometrical characterization of the Avilé Member with well data (black dots mark the position of wells). (A) Wireline log indicating top and base of Avilé Mb, and position of the *datum* surface. (B) Thickness map between *datum* and Avilé top. (C) Dip angle map derived from the surface shown at Fig. 9B. (D) Dip azimuth map derived from the surface shown at Fig. 9B. See text for comparisons and interpretations.

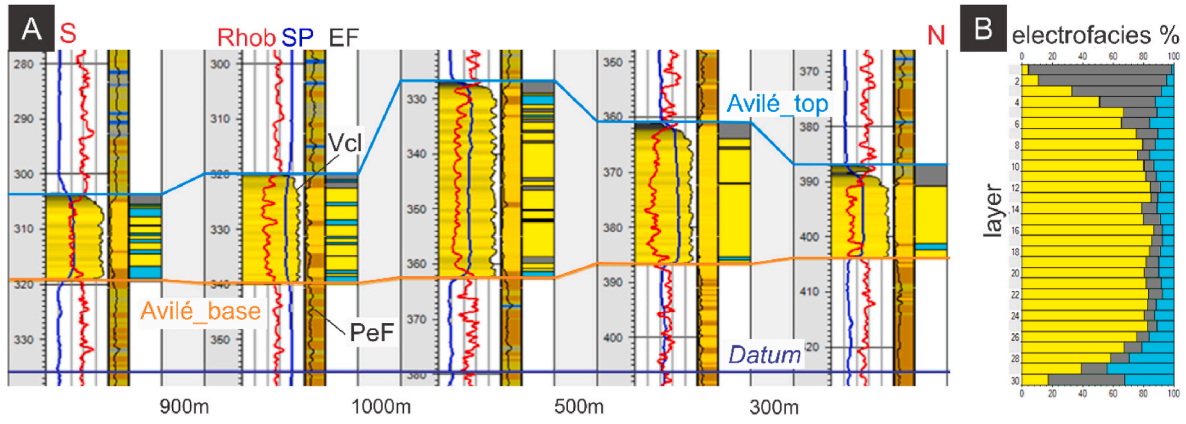

Fig. 9. Spatial variations in electrofacies. Color scheme is the same as in Fig. 5 and Table 1 (A) Section perpendicular to preserved megadune orientation (see location in Fig. 8B). There are no obvious lateral variations in electrofacies coupled with variation in thickness (PeF = photoelectric absorption factor wireline log; Vcl = clay volume, calculated from GR wireline log). (B) Vertical variations in electrofacies in wells across the whole study area. (For interpretation of the references to color in this figure legend, the reader is referred to the Web version of this article.)

development of water influenced or water-lain accumulation (*i.e.* stokes surfaces). The water table had gradually more influence over sedimentation until the sand sea died in the area and a fluvial system developed.

The eolian record is known to be continuous between the Pampa de Tril outcrops and the study area (Valenzuela, 2002), indicating they must have been part of the same sand sea. Thus, the evolution of the eolian system in Puesto Hernandez Field likely followed a similar evolution as was interpreted in the outcrops, but in a more downwind or erg center position. It follows then that the formation of damp to subaqueous deposits (FA-B, EF-2) and more importantly, of carbonate cemented horizons (EF-3) was most likely the result of supersurface formation by deflation down to the water table. The formation of thicker, and more abundant carbonate cementation in comparison to the less abundant water-lain or water influenced facies, seem to be evidence

in favor of this interpretation in the lowermost, accumulated interval of the Avilé Member. This would further explain reduced petrophysical properties in the interdune areas, since the whole record in these areas is composed of only by the accumulated interval, characterized by these cemented horizons.

7.3. Sequence stratigraphic model

The gathered information allows us to suggest a sequence stratigraphic model for accumulation of the unit in the study area (Fig. 10). The sudden retreat of the Neuquén Sea provoked erosion of previous marine deposits, probably by the action of fluvial systems, which left no distinctive fluvial deposits in this area given their low accommodation conditions far from the basin center. The result of this stage is the formation of a low relief (2–4 m) erosion surface at the base of the Avilé Member, interpreted by previous authors in other localities as a sequence boundary (Legarreta, 2002; Veiga et al., 2007).

The accumulation of continental deposits in the area is thought to have been related to several episodes of eolian sand sea construction, accumulation, and partial deflation down to the water table. Abundant sand supply, only available when dryer conditions prevailed in the ephemeral fluvial systems to the west and southwest (Veiga et al., 2011), coupled with strong winds in the north-northeast and east direction (Veiga et al., 2007), allowed for the construction and accumulation of the Avilé Dunefield (Fig. 10A). Events of deflation down to the water table led to the accumulation of thin water-lain or water table influenced deposits and the formation of cemented horizons (Fig. 10B). In comparison to the outcrops 90 km to the west, here the water-lain or damp deposits were much less developed, because of the position close or slightly downwind to the erg center. Hence, the most striking characteristic of super surfaces in Puesto Hernández Field are the formation of cemented horizons, which, although thin, could be laterally extensive. The result of this stage is the accumulated interval of the Avilé Member, which are the lowermost 5–10 m. This eolian accumulation was most likely preserved by 'normal' (water table rise) mechanisms (Kocurek, 1999).

The last stage of continental deposition of the Avilé Member (Fig. 10C) is characterized by the construction of large linear megadunes. Although representing very little time in comparison to previous stage, it makes up for most of the record in volume of the Avilé Member. The result of this stage is the non-accumulated interval of the Avilé Member, found in uppermost meters of the unit in the megadune sectors and thinning almost completely in the interdune sectors.

Finally, the linear dunes were flooded and preserved by the sudden transgression Neuquén Sea (Fig. 10D), marking the end of lowstand conditions in the area (Veiga et al., 2007). No evidence was found to suggest accumulation under a transgressive system track before the actual flooding in the studied area. Flooding provoked the destabilization, deformation and reworking of dune sand, putting the megadunes below the regional level of erosion. The result of this stage is the discrete interval of marine reworked elements in the uppermost meters of the Avilé Member in megadune flank and interdune sectors, separated from the eolian deposits by a transgressive surface.

8. Geocellular modelling

The workflow presented here for geocellular modeling is based on modeling the accumulated and the non-accumulated eolian intervals (*sensu* Kocurek, 1999) of the Avilé Member as different zones. A geometric method was developed to map the accumulation surface that bounds the two intervals. The rationale backing this method comes from: (i) accumulated intervals have a sedimentary architecture of a climbing bedform system, very different to that of non-accumulated, preserved bedforms, (ii) the Avilé Member's accumulated interval likely contains extensive super-surfaces, which control the position of carbonate cemented horizons and water-lain facies of impoverished reservoir quality (local baffles and barriers to flow); which would not be expected in non-accumulated interval (which was well above water table level when dunes were active) and (iii) accumulated intervals most certainly contain interdune facies of different types, which are not found in the non-accumulated interval.

The accumulation surface is an imaginary horizon that links interdune lows and separates accumulated sediment below from in transport sediment above (Middleton and Southard, 1984, Mountney, 2012). To map the accumulation surface, the lowermost points across the interdune lows were picked, and later interpolated using the Pilmatué Member *datum* as a surface trend (Fig. 11A). The mapping was refined until it filled the expectations for this surface (Fig. 11B).

Separating these two zones inside the Avilé Member allowed to differentiate EF-2 as water-lain or damp elements in the accumulated interval (EF-2a), and as marine reworking elements in the non-accumulated interval (EF-2b). This was helpful to set variograms for facies modelling that satisfied our expectations of the dimensions of these elements. From our outcrop analogues, we expect marine

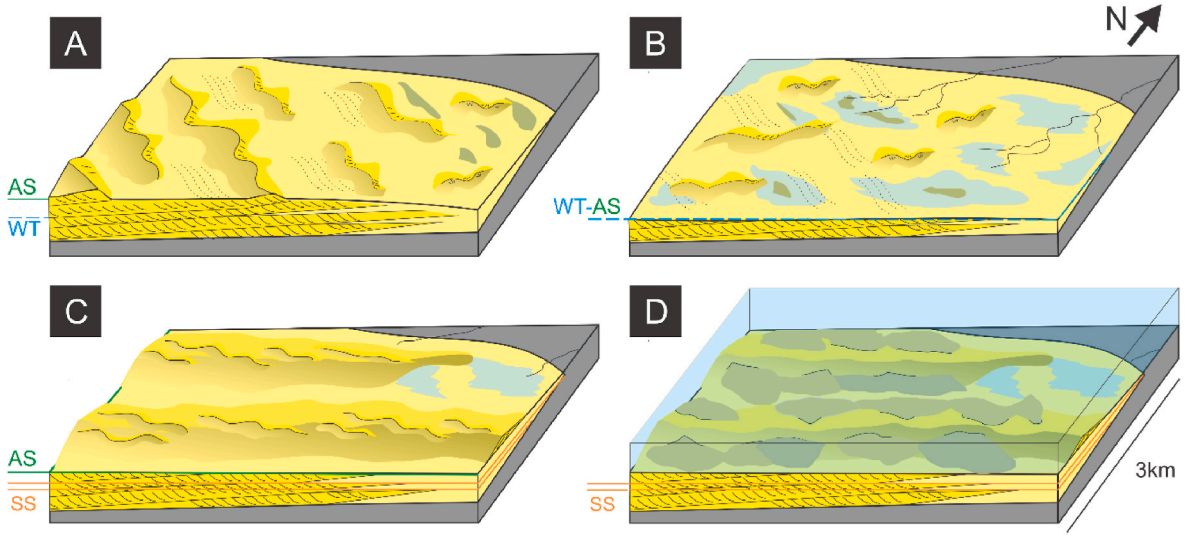

Fig. 10. Conceptual model of the accumulation systems for the Avilé Member in the study area and their evolution in time. (AS = accumulation surface; WT = water table) (A) Episodes of construction and accumulation of eolian sequences. (B) Deflation episodes down to the water table. Generation of super surfaces (SS). (C) Situation before marine transgression, characterized by large linear megadunes oriented E-W. (D) Flooding and reworking of the megadunes by the Neuquén Sea.

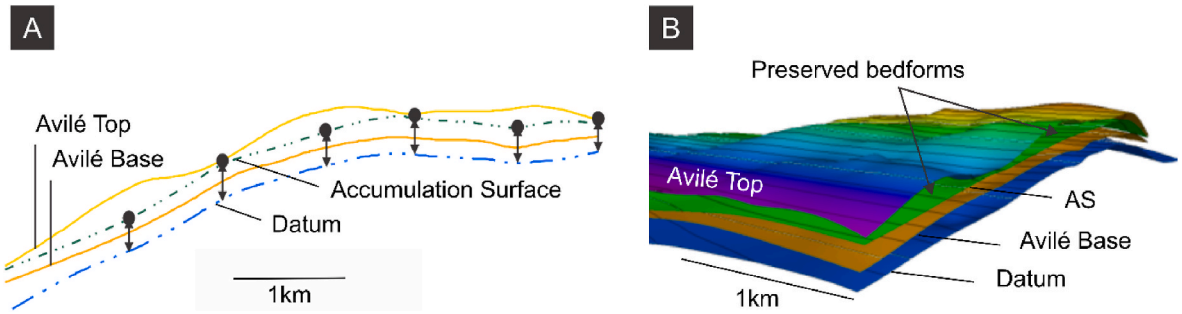

Fig. 11. Zoning workflow. (A) Mapping of accumulated and not-accumulated intervals as different zones was performed by joining interdune lows and using the *datum* surface as a trend. (B) The mapped accumulation surface (AS) was evaluated and modified until it fit both data and geological concept.

reworking elements for example to be very continuous sheets, with a correlation length superior to inter-well distance, while water-lain, or damp elements are expected to have a correlation length less than inter-well distance. The resulting geocellular model was compared to conceptual geological block models, suggesting a good representation of the geological concepts (Fig. 12). The model was also successful in history matching of the field, once overall petrophysical variables (K, Phi) were adjusted.

9. Discussion

The development of a conceptual model consistent with eolian sequence stratigraphic concepts (Kocurek and Havholm, 1993; Kocurek, 1999), and the identification of accumulated and non-accumulated intervals had a profound impact on how the reservoir was interpreted, characterized, and modelled. Before the development of this model, it was very tempting to link lateral variations in seismic properties to lateral variations in porosity (Dolberg et al., 2000) controlled by facies. In this way, poorer overall properties in the interdune sector could have been explained by the corresponding presence of interdune facies (Fig. 13A). In contrast, the conceptual model proposed in this study (Fig. 13B) explains variations in overall seismic properties in the dune and interdune sectors by: (i) the thinning of the non-accumulated interval in the interdune sector, which is free of interdune and extensive

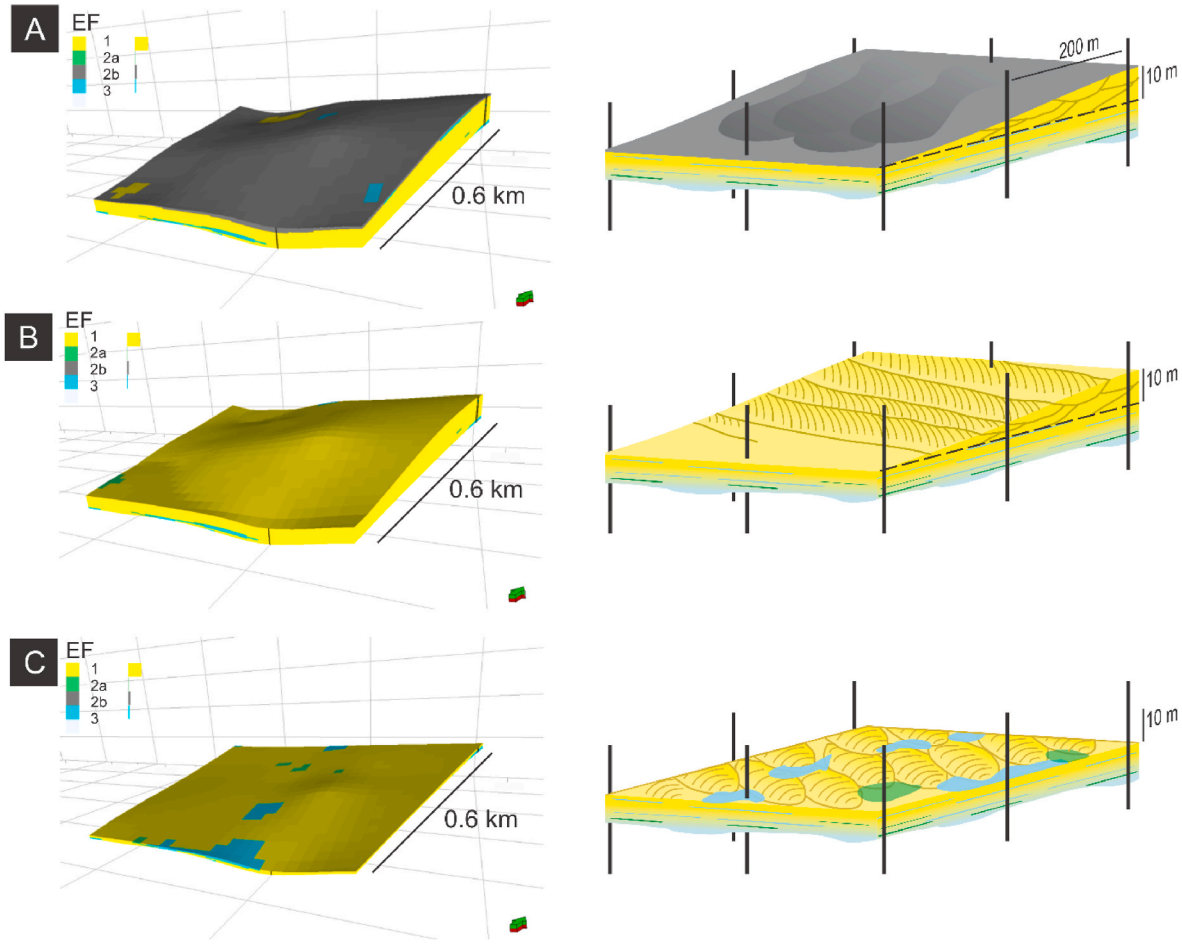

Fig. 12. Facies modelling results in 3D view for each interval (left), compared to the conceptual model (right). (A) Top of the marine reworked interval, characterized by extensive marine reworking elements. (B) The non-accumulated interval, with the most homogeneous facies and petrophysical properties. (C) The accumulated interval. Characterized by favorable facies interbedded with cemented horizons and water-lain or damp elements (EF-2).

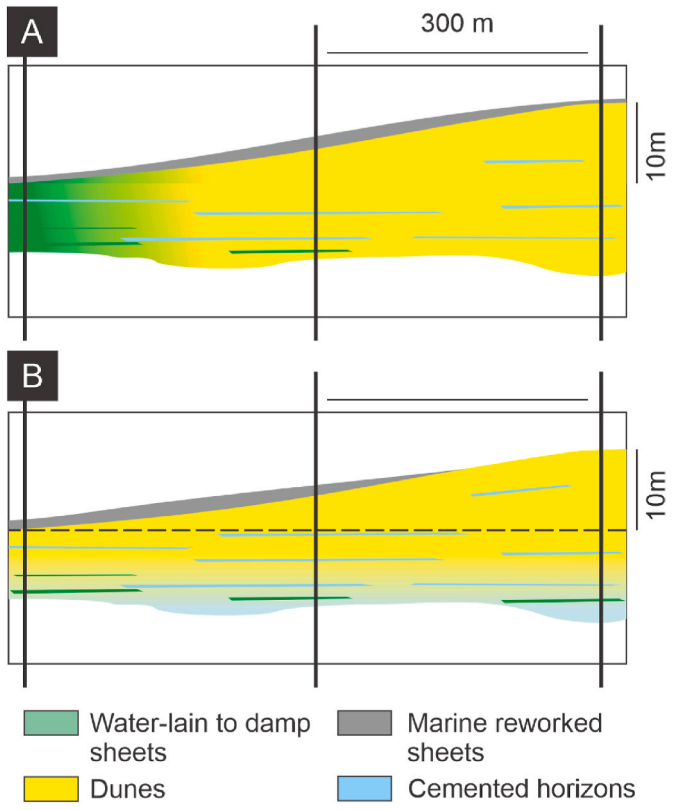

Fig. 13. Different conceptual models that account for facies distribution and contrasting seismic properties in megadune and interdune areas. (A) Lateral variation concept: facies are controlled by preserved topography (*i.e.* interdune sectors correlate to interdune facies). (B) Vertical variation or zoning concept: facies distribution is controlled by intervals with distinct accumulation conditions, and the thickness of such intervals affect overall reservoir properties.

cemented horizons representing overall better reservoir conditions; and (ii) the thickening of marine reworking deposits towards the lower dune flanks and interdunes.

Changes in zoning with the workflow presented in this study had considerable impact in the resulting reservoir model. Comparing our proposed geocelullar model to a one-zone model (Fig. 14) highlights the impact of this workflow. Firstly, interpolation of facies changes dramatically. In a one zone model, elements from the accumulated interval could be extrapolated into the non-accumulated sector, resulting in a very different geometry of sedimentary heterogeneity. This is not consistent with our conceptual model, which fits better with the presence of two zones with independent interpolation. Furthermore, having two zones (for accumulated and non-accumulated intervals respectively) allowed representing the expected dimensions of modeling elements in each interval, and that had a remarkable difference in the extension of buffers and barriers to flow.

Numerous outcrop analog studies have supported the definition of reservoir zones based on stratigraphic cycles in the case of marginal eolian reservoirs, where eolian facies are interbedded with non-eolian facies associations like fluvial and sabkha (Sweet et al., 1996; Veiga et al., 2002; Mountney and Jagger, 2004; Taggart et al., 2010). Other studies have focused on modeling the hierarchies of bounding surfaces within the record of a climbing dune system (Ciftci et al., 2004; Fischer et al., 2007) and modeling of sedimentary bodies and their internal heterogeneities (Cox et al., 1994; Romain and Mountney, 2014). However, no suggestion for zoning a reservoir model based on the differences between accumulated and non-accumulated intervals has been proposed. The workflow presented in this study is one possible way of considering such intervals for reservoir zoning in the numerous cases worldwide (*e.g.* Norphlet Sandtone in the Gulf of Mexico, Rotliegend Group in the North Sea, Tordillo Formation and Troncoso Member in the Neuquén Basin, among many others) that are known to have preservation of topography (Strömbäck and Howell, 2002; Cevallos, 2005; Dajczgewand et al., 2006; Ajdukiewicz et al., 2010).

The key impact that the distribution of facies and bounding surfaces, conditioned by sedimentary and stratigraphic architecture, have in eolian reservoir properties is well known (Chandler et al., 1989; Fischer et al., 2007, Taggart et al., 2010). Therefore, considering the presented differences between accumulated and non-accumulated intervals, their identification will very likely have significant advantages to model any eolian reservoir with preserved bedforms (Fig. 15). Regardless if the accumulated interval is made up of (i) the stacking of previous sequences (Fig. 15A; *e.g.* Avilé Member; Veiga et al., 2002; Leman

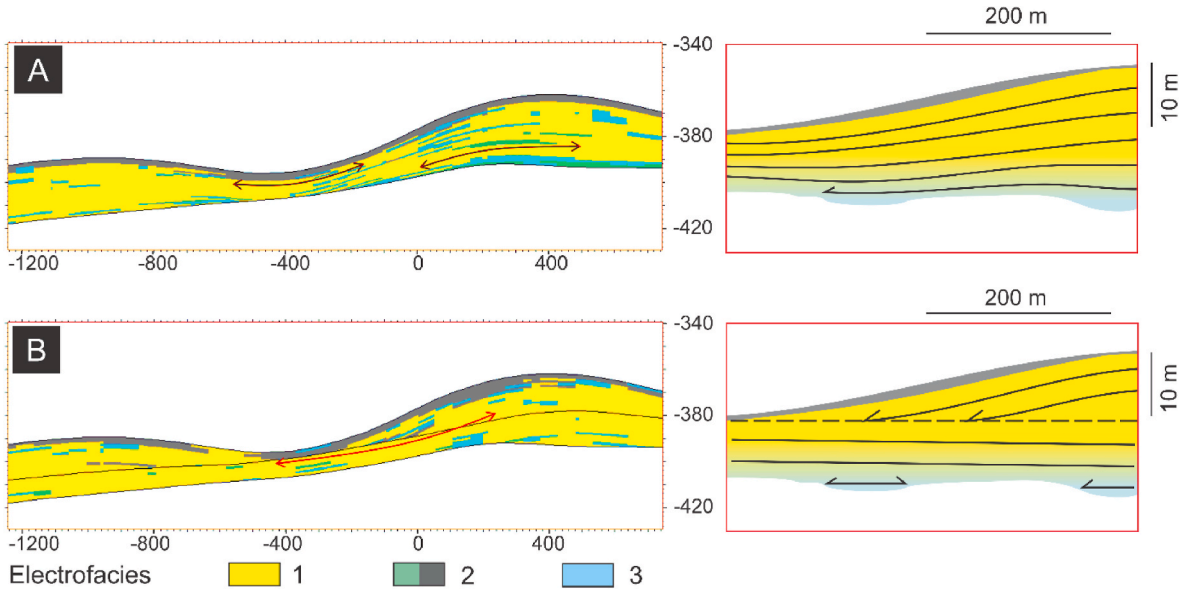

Fig. 14. Facies modeling results. (A) One zone model, top and base conform. The one zone model provides interpolation results that don't match the conceptual model (*e.g.*, we wouldn't expect facies in the non-accumulated interval to correlate to the accumulated interval). (B) Two zone model, both non-accumulated and accumulated intervals are top conform with fixed cell height. Interpolation of facies results is more accurate in this model.

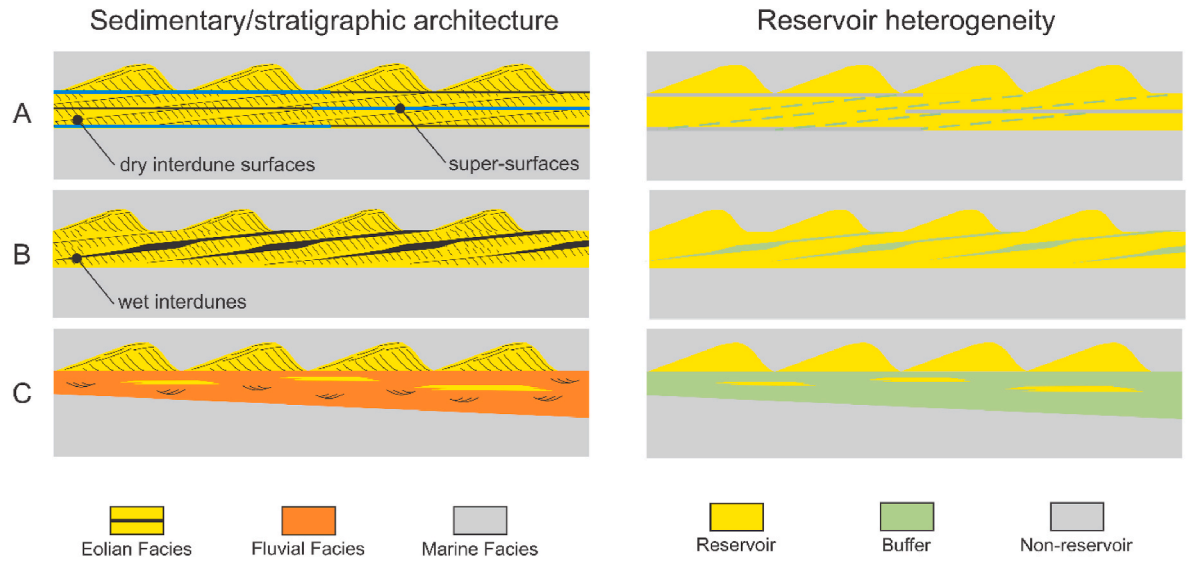

Fig. 15. Different scenarios of eolian successions with preserved bedforms or non-accumulated intervals, and their expected reservoir heterogeneity. (A) Dry system with multiple stages of accumulation and deflation, and the formation of super surfaces (*e.g.* Avilé Member; Rotliegend Group). (B) Wet system with one single accumulation stage (*e.g.* Tordillo Formation). (C) Dry system with no accumulation stage (*e.g.* Troncoso Inferior Member).

Sandstone of the Rotliegend Group; Howell and Mountney, 1997; Strömbäck and Howell, 2002), (ii) the same sequence as the preserved bedform interval (Fig. 15B; likely case of Tordillo Formation; Cevallos, 2005; Veiga and Spalletti, 2007) or (iii) the record of a different sedimentary system (Fig. 15C; Troncoso Member; Argüello Scotti and Veiga, 2019), the non-accumulated interval is likely going to portray a distinctive sedimentary architecture that suggests its separation as a zone within the reservoir. Considering the uncertainty that geologists face when dealing with the subsurface, it is helpful to know that differences in sedimentary architecture between accumulated and non-accumulated intervals are to be expected and can have a profound impact on fluid flow.

10. Conclusions

This study presents a workflow that was successful in identifying, mapping, and modelling accumulated and non-accumulated eolian intervals within the Avilé Member in the Puesto Hernandez Field. A conceptual model was developed from field data and based on eolian sequence stratigraphic concepts. This model showed how accumulated and non-accumulated intervals in the Avilé Member have contrasting styles of petrophysical heterogeneity, given that each interval is characterized by (i) the presence or absence of modeling elements (ii) the different dimensions and geometry of such modeling elements (iii) contrasting early diagenetic conditions. A geocelullar modelling workflow based on the mapping of the ancient accumulation surface was successful in representing both intervals as different model zones. This methodology is shown to have a provide a good representation of geological concepts and to have an impact in the expected reservoir heterogeneity. Hypothetical scenarios for other successions are presented, showing how these concepts and methodology may be relevant for modeling other eolian and fluvio-eolian reservoirs around the world.

Declaration of competing interest

The authors declare that they have no known competing financial interests or personal relationships that could have appeared to influence the work reported in this paper.

Data availability

The authors do not have permission to share data.

Aknowledgements

The authors would like to express their acknowledgements to YPF S. A. for the permission to publish the details of this study. Comments and suggestions from reviewer Juan Pedro Rodríguez-Lopez were key to improving this manuscript to its final version.

References

Argüello, J., 2011. Yacimiento Puesto Hernández. In: Leanza, H.A., Arregui, C., Carbone, O., Danieli, J.C., Vallés, J.M. (Eds.), Relatorio del XVIII Congreso Geológico Argentino, pp. 663–667.

Ajdukiewicz, J.M., Nicholson, P.H., Esch, W.L., 2010. Prediction of deep reservoir quality using early diagenetic process models in the Jurassic Norphlet Formation, Gulf of Mexico. AAPG (Am. Assoc. Pet. Geol.) Bull. 94, 1189–1227. https://doi.org/10.1306/04211009152.

Argüello Scotti, A., Veiga, G.D., 2015. Morphological characterization of an exceptionally preserved eolian system: the cretaceous Troncoso inferior member in the Neuquén Basin (Argentina). Lat. Am. J. Sedimentol. Basin Anal. 22, 29–46.

Argüello Scotti, A., Veiga, G.D., 2019. Sedimentary architecture of an ancient linear megadune (Barremian, Neuquén Basin): insights into the long-term development and evolution of aeolian linear bedforms. Sedimentology 66, 2191–2213. https://doi.org/10.1111/sed.12597.

Benan, C.A.A., Kocurek, G., 2000. Catastrophic flooding of an eolian dune field: jurassic entrada and todilto formations, ghost ranch, New Mexico, USA. Sedimentology 47, 1069–1080. https://doi.org/10.1046/j.1365-3091.2000.00341.x.

Besly, B., Romain, H.G., Mountney, N.P., 2018. Reconstruction of linear dunes from ancient eolian successions using subsurface data: permian Auk Formation, Central North Sea, UK. Mar. Petrol. Geol. 91, 1–18. https://doi.org/10.1016/j.marpetgeo.2017.12.02.

Bristow, C.S., Pugh, J., Goodall, T., 1996. Internal structure of eolian dunes in Abu Dhabi determined using ground-penetrating radar. Sedimentology 43, 995–1003. https://doi.org/10.1111/j.1365-3091.1996.tb01515.x.

Bristow, C.S., Bailey, S.D., Lancaster, N., 2000. The sedimentary structure of linear sand dunes. Nature 406, 56–59. https://doi.org/10.1038/35017536.

Chandler, M.A., Kocurek, G., Goggin, D.J., Lake, L.W., 1989. Effects of stratigraphic heterogeneity on permeability in eolian sandstone sequence, Page Sandstone, Northern Arizona. AAPG Bull. 73, 658–668. https://doi.org/10.1306/44B4A249-170A-11D7-8645000102C1865D.

Ciftci, B.N., Aviantara, A.A., Hurley, N.F., Kerr, D.R., 2004. Outcrop-based three-dimensional modeling of the tensleep sandstone at alkali creek, bighorn basin, Wyoming. In: Grammar, G.M., Harris, P.M., Eberli, G.P. (Eds.), Integration of Outcrop and Modern Analogs in Reservoir Modeling, pp. 235–259. https://doi.org/10.1306/M80924C12.

Cevallos, M., 2005. Análisis estratigráfico de alta frecuencia del límite kimmeridgiano-tithoniano en el subsuelo de la Dorsal de Huincul, Cuenca Neuquina. Petrotecnia. December 34–55.
Clemmensen, L.B., 1989. Preservation of interdraa and plinth deposits by the lateral migration of large linear draas (Lower Permian Yellow Sands, northeast England). Sediment. Geol. 65, 139–151. https://doi.org/10.1016/0037-0738(89)90011-0.
Cox, D.L., Lindquist, S.J., Bargas, C.L., Havholm, K.G., Srivastava, R.M., 1994. Integrated Modeling for Optimum Management of a Giant Gas Condensate Reservoir, Jurassic Eolian Nugget Sandstone, Anschutz Ranch East Field, Utah Overthrust (U.S.A.). In: Yarus, J.M., Chambers, R.L. (Eds.), Stochastic Modeling and Geostatistics: Principles, Methods, and Case Studies, AAPG Computer Applications in Geology, pp. 287–321. https://doi.org/10.1306/CA3590C22. No. 3.
Dajczgewand, D., Nocioni, A., Fantin, M., Minniti, S., Calegari, R., Gavarrino, A., 2006. Lower Troncoso Eolian Bodies Identification in the Neuquén Basin, Argentina: A Different Approach and some Geological Implications. In: 9th Simposio Bolivariano - Exploración Petrolera en las Cuencas Subandinas. https://doi.org/10.3997/2214-4609-pdb.111.145.
Dolberg, D.M., Helgesen, J., Hanssen, T.H., Magnus, I., Saigal, G., Pedersen, B.K., 2000. Porosity prediction from seismic inversion, Lavrans Field, Halten Terrace, Norway. Lead. Edge 19, 392–399. https://doi.org/10.1190/1.1438618.
Fielding, C., 2006. Upper flow regime sheets, lenses and scour fills: Extending the range of architectural elements for fluvial sediment bodies. Sediment. Geol. 190, 227–240. https://doi.org/10.1016/j.sedgeo.2006.05.009.
Fischer, C., Gaupp, R., Dimke, M., Sill, O., 2007. A 3D high resolution model of bounding surfaces in aeolian-fluvial deposits: An outcrop analogue study from the Permian Rotliegend, Northern Germany. J. Petrol. Geol. 30, 257–273. https://doi.org/10.1111/j.1747-5457.2007.00257.x.
Franzese, J., Spalletti, L., Pérez, I.G., Macdonald, D., 2003. Tectonic and paleoenvironmental evolution of Mesozoic sedimentary basins along the Andean foothills of Argentina (32°-54°S). J. S. Am. Earth Sci. 16, 81–90. https://doi.org/10.1016/S0895-9811(03)00020-8.
Ford, C., Bryant, G., Nick, K.E., 2016. Architectural evidence of dune collapse in the Navajo sandstone, zion national Park, Utah. Sediment. Geol. 344, 222–236. https://doi.org/10.1016/j.sedgeo.2016.04.009.
Fryberger, S.G., Dean, G., 1979a. Dune forms and wind regime. In: McKee, E.D. (Ed.), A Study of Global Sand Seas. United States Geological Survey Professional Paper 1052, pp. 137–170. https://doi.org/10.3133/pp1052.
Fryberger, S.G., Schenk, C.J., Krystinik, L.F., 1988. Stokes surfaces and the effects of near-surface groundwater-table on eolian deposition. Sedimentology 35, 21–41. https://doi.org/10.1111/j.1365-3091.1988.tb00903.x.
Fryberger, S.G., Dean, G., 1979b. Dune forms and wind regime. In: McKee, E.D. (Ed.), A Study of Global Sand Seas. U.S. Government Printing Office, Washington, D.C, pp. 137–169. https://doi.org/10.3133/pp1052. Professional Paper No. 1052.
Fryberger, S.G., Knight, R., Hern, C., Moscariello, A., Kabel, S., 2011. Rotliegend Facies, Sedimentary Provinces, and Stratigraphy, Southern Permian Basin Uk and the Netherlands: A Review with New Observations. In: Grötsch, J., Gaupp, R. (Eds.), The Permian Rotliegend of the, pp. 51–88. https://doi.org/10.2110/pec.11.98.0051. Netherlands.
Glennie, K.W., Buller, A.T., 1983. The Permian Weissliegend of NW Europe—the partial deformation of eolian dune sands caused by the Zechstein Transgression. Sediment. Geol. 35, 43–81. https://doi.org/10.1016/0037-0738(83)90069-6.
Howell, J., Mountney, N., 2001. Eolian grain flow architecture: hard data for reservoir models and implications for red bed sequence stratigraphy. Petrol. Geosci. 7, 51–56. https://doi.org/10.1144/petgeo.7.1.51.
Howell, J.A., Mountney, N.P., 1997. Climatic cyclicity and accommodation space in arid and semi-arid depositional systems: an example from the Rotliegende Group of the southern North Sea. In: North, C.P., Prosser, J.D. (Eds.), Petroleum Geology of the Southern North Sea: Future Potential. Geological Society, London, Special Publications No. 123, pp. 199–218. https://doi.org/10.1144/GSL.SP.1997.123.01.05.
Howell, J.A., Schwarz, E., Spalletti, L.A., Veiga, G.D., 2005. The Neuquén Basin: an overview. In: Veiga, G.D., Spalletti, L.A., Howell, J.A., Schwarz, E. (Eds.), The Neuquén Basin, Argentina: A Case Study in Sequence Stratigraphy and Basin Dynamics. Special Publication 252. Geological Society of London, pp. 1–14. https://doi.org/10.1144/GSL.SP.2005.252.01.01.
Hunter, R.E., 1977. Basic types of stratification in small eolian dunes. Sedimentology 24, 361–387. https://doi.org/10.1111/j.1365-3091.1977.tb00128.x.
Jerram, D.A., Mountney, N.P., Howell, J.A., Long, D., Stollhofen, H., 2000. Death of a sand sea: an active eolian erg systematically buried by the Etendeka flood basalts of NW Namibia. J. Geol. Soc. 157, 513–516. https://doi.org/10.1144/jgs.157.3.513.
Kocurek, G., 1981. Significance of interdune deposits and bounding surfaces in eolian dune sands. Sedimentology 28, 753–780. https://doi.org/10.1111/j.1365-3091.1981.tb01941.x.
Kocurek, G., 1988. First-order and super bounding surfaces in eolian sequences -Bounding surfaces revisited. Sediment. Geol. 56, 193–206. https://doi.org/10.1016/0037-0738(88)90054-1.
Kocurek, G., 1999. The eolian rock record (Yes, Virgina, it exists, but it really is rather special to create one). In: Goudie, A.S., Livingstone, I., Stokes, S. (Eds.), Eolian Environments Sediments and Landforms. John Wiley and Sons, Chichester, pp. 239–259.
Kocurek, G., Dott, R.H., 1981. Distinctions and Uses of Stratification Types in the Interpretation of Eolian Sand. J. Sediment. Res. 51, 579–595. https://doi.org/10.1306/212F7CE3-2B24-11D7-8648000102C1865D.
Kocurek, G., Havholm, K.G., 1993. Eolian sequence stratigraphy— a conceptual framework. In: Weimer, P., Posamentier, H.W. (Eds.), Siciliclastic Sequence Stratigraphy. American Association of Petroleum Geologists, Memoir 58, pp. 393–409.
Kocurek, G., Fielder, G., 1982. Adhesion structures. J. Sediment. Petrol. 52, 1229–1241.
Lancaster, N., 1995. Geomorphology of Desert Dunes. Routledge, London. https://doi.org/10.1017/S0016756800008931.
Legarreta, L., 2002. Eventos de desecación en la Cuenca Neuquina: depósitos continentales y distribución de hidrocarburos. In: V Congreso de Exploración y Desarrollo de Hidrocarburos. Instituto Argentino del Petróleo y Gas, Mar del Plata, Argentina.
Leanza, H.A., 2009. Las principales discontinuidades del Mesozoico de la cuenca Neuquina según observaciones de superficie. Rev. Mus. Argent. Ciencias Nat. Nueva Ser. 11 (2), 145–184.
Lowe, D.R., 1976. Subaqueous liquefied and fluidized sediment flows and their deposits. Sedimentology 23, 285–308. https://doi.org/10.1111/j.1365-3091.1976.tb00051.x.
Lowe, D.R., LoPiccolo, R.D., 1974. The characteristics and origins of dish and pillar structures. J. Sediment. Petrol. 44, 484–501. https://doi.org/10.1306/74D72A68-2B21-11D7-8648000102C1865D.
McKee, E.D., 1979. A Study of Global Sand Seas, vol. 1052. Professional Paper, Reston, VA, pp. 399–407. https://doi.org/10.3133/pp1052. US Geological Survey.
Middleton, G.V., Southard, J.B., 1984. Mechanics of sediment movement. SEPM Short. Course 3.
Mitchum, R.M., Uliana, M.A., 1985. Seismic stratigraphy of carbonate depositional sequences. Upper Jurassic/Lower Cretaceous. Neuquén Basin, Argentina. In: Berg, B. R., Woolverton, D.G. (Eds.), Seismic Stratigraphy, II. An Integrated Approach to Hydrocarbon Analysis, vol. 39. AAPG Memoir, pp. 255–274.
Mountney, N.P., 2012. A stratigraphic model to account for complexity in eolian dune and interdune successions. Sedimentology 59, 964–989. https://doi.org/10.1111/j.1365-3091.2011.01287.x.
Mountney, N.P., Howell, J.A., 2000. Eolian architecture, bedform climbing and preservation space in the Cretaceous Etjo Formation, NW Namibia. Sedimentology 47, 825–849. https://doi.org/10.1046/j.1365-3091.2000.00318.x.
Mountney, N.P., Howell, J.A., Flint, S.S., Jerram, D.A., 1999. Climate, sediment supply and tectonics as controls on the deposition and preservation of the eolian-fluvial Etjo Sandstone Formation, Namibia. J. Geol. Soc. 156, 771–779. https://doi.org/10.1144/gsjgs.156.4.0771.
Mountney, N.P., Jagger, A., 2004. Stratigraphic evolution of an eolian erg margin system: the Permian Cedar Mesa Sandstone, SE Utah, USA. Sedimentology 51, 713–743. https://doi.org/10.1111/j.1365-3091.2004.00646.x.
Pramparo, M.B., Vokheimer, W., 2014. Palinología del Miembro Avilé (Formación Agrio, Cretácico Inferior) en el cerro de la Parva, Neuquén. Ameghiniana 56 (2), 217–227.
Rodríguez-López, J.P., Clemmensen, L.B., Lancaster, N., Mountney, N.P., Veiga, G.D., 2014. Archean to Recent aeolian sand systems and their sedimentary record: Current understanding and future prospects. Sedimentology 61, 1487–1534. https://doi.org/10.1111/sed.12123.
Rodríguez-López, J.P., Wu, C., 2020. Recurrent deformations of aeolian desert dunes in the cretaceous of the South China Block: Trigger mechanisms variability and implications for aeolian reservoirs. Mar. Petrol. Geol. 119 https://doi.org/10.1016/j.marpetgeo.2020.104483.
Romain, H.G., Mountney, N.P., 2014. Reconstruction of three-dimensional eolian dune architecture from one-dimensional core data through adoption of analog data from outcrop. AAPG (Am. Assoc. Pet. Geol.) Bull. 98, 1–22. https://doi.org/10.1306/05201312109.
Rubin, D.M., Hunter, R.E., 1982. Bedform climbing in theory and nature. Sedimentology 29, 121–138. https://doi.org/10.1111/j.1365-3091.1982.tb01714.x.
Scherer, C.M.S., 2002. Preservation of eolian genetic units by lava flows in the Lower Cretaceous of the Paraná Basin, southern Brazil. Sedimentology 49, 97–116. https://doi.org/10.1046/j.1365-3091.2002.00434.x.
Sweet, M.L., Blewden, C.J., Carter, A.M., Mills, C.A., 1996. Modelling heterogeneity in a low permeability gas reservoir using geostatistical techniques, Hyde Field, Southern North Sea. AAPG Bull. 80, 1719–1735. https://doi.org/10.1306/64EDA14A-1724-11D7-8645000102C1865D.
Strömbäck, A., Howell, J.A., 2002. Predicting distribution of remobilized eolian facies using sub-surface data: the Weissliegend of the UK Southern North Sea. Petrol. Geosci. 8, 237–249. https://doi.org/10.1144/petgeo.8.3.237.
Strömbäck, A., Howell, J.A., Veiga, G.D., 2005. The transgression of an erg-sedimentation and reworking/soft-sediment deformation of eolian facies: the Cretaceous Troncoso Member, Neuquén Basin, Argentina. In: Veiga, G.D., Spalletti, L.A., Howell, J.A., Schwarz, E. (Eds.), The Neuquén Basin, Argentina: A Case Study in Sequence Stratigraphy and Basin Dynamics. Special Publication 252. The Geological Society of London, London, pp. 163–183. https://doi.org/10.1144/GSL.SP.2005.252.01.08.
Taggart, S., Hampson, G.J., Jackson, M.D., 2010. High-resolution stratigraphic architecture and lithological heterogeneity within marginal eolian reservoir analogues. Sedimentology 57, 1246–1279. https://doi.org/10.1111/j.1365-3091.2010.01145.x.
Valenzuela, M., 2002. Los Reservorios del Miembro Avilé de la Formación Agrio. In: Schiuma, M., Hinterwimmer, G., Vergani, G. (Eds.), Rocas Reservorio de las Cuenca Productivas de la Argentina. IAPG, pp. 433–442.
Veiga, G.D., Spalleti, L.A., 2007. The Upper Jurassic (Kimmeridgian) fluvial–aeolian systems of the southern Neuquén Basin, Argentina. Gondwana Res. 11, 286–302. https://doi.org/10.1016/j.gr.2006.05.002.
Veiga, G.D., Spalletti, L.A., Flint, S.S., 2002. Eolian/fluvial interactions and high-resolution sequence stratigraphy of a non-marine lowstand wedge: the Avilé Member of the Agrio Formation (Lower Cretaceous), central Neuquén Basin, Argentina. Sedimentology 49, 1001–1019. https://doi.org/10.1046/j.1365-3091.2002.00487.x.

Veiga, G.D., Spalletti, L.A., Flint, S.S., 2007. Anatomy of a fluvial lowstand wedge: the Avilé Member of the Agrio Formation (Hauterivian) in central Neuquén Basin (NW Neuquén province), Argentina. In: Nichols, G., Williams, E., Paola, C. (Eds.), Sedimentary Environments, Processes and Basins. A Tribute to Peter Friend, vol. 38. Special Publication International Association of Sedimentologists, pp. 341–365. https://doi.org/10.1002/9781444304411.ch16.

Veiga, G.D., Spalletti, L.A., Schwarz, E., 2011. El Miembro Avilé de la Formación Agrio (Cretácico Temprano). In: Leanza, H.A., Arregui, C., Carbone, O., Danieli, J.C., Vallés, J.M. (Eds.), Geología y Recursos Naturales de la Provincia del Neuquén, pp. 161–173.

Weaver, C.E., 1931. Paleontology of the Jurassic and Cretaceous of West Central Argentina, vol. 1. Memoir University of Washington.